ERJ Express. Published on July 7, 2011 as doi: 10.1183/09031936.00141010

Parenchymal trafficking of pleural mesothelial cells in idiopathic pulmonary fibrosis

Kamal K. Mubarak,[1] Ana Montes-Worboys,[1] Doron Regev,[1] Najmunnisa Nasreen,[1,2] Kamal A. Mohammed,[1,2] Ibrahim Faruqi,[1] Edward Hensel,[1] Maher A. Baz,[1] Olufemi A. Akindipe,[1] Sebastian Fernandez-Bussy,[1] Steven D. Nathan,[3] and Veena B. Antony[4]

[1]Division of Pulmonary, Critical Care Medicine, and Sleep Medicine, Department of Medicine, College of Medicine, University of Florida, PO Box 100225, Gainesville, FL 32610-0225

[2]Malcolm Randall VA Medical Center, Gainesville, FL 32608

[3]Advanced Lung Disease and Transplant Program, Inova Heart and Vascular Institute, Inova Fairfax Hospital, 3300 Gallows Road, Falls Church, VA 22046

[4]Division of Pulmonary, Allergy and Critical Care Medicine, Departments of Medicine and Environmental Health Sciences, 1530 3rd Avenue South THT 413, Birmingham, AL 35294-0006

Address for Correspondence: Kamal K. Mubarak, MD
Division of Pulmonary, Critical Care Medicine and Sleep Medicine, Department of Medicine, College of Medicine, University of Florida, P.O. Box 100225, Gainesville, FL 32610. Tel: (352) 273-8740. Fax: (352) 392-0821. E-mail: kamal.mubarak@gmail.com

Running Title: Pleural mesothelial trafficking in IPF

ACKNOWLEDGEMENTS

We would like to acknowledge the kindness of Mrs Carole McCall. Secretarial support was provided by Christine Dämm, Patricia Perry, and LaSonya Owens. This work was supported by NIH grants R21AA014796 and R01AI080349 to VBA.

ABSTRACT

RATIONALE: Idiopathic pulmonary fibrosis (IPF) is characterized by myofibroblast proliferation leading to architectural destruction. Neither the origin nor the continued proliferation of myofibroblasts is well understood.

METHODS: Explanted human IPF lungs were stained by immunohistochemistry for calretinin, a marker of pleural mesothelial cells (PMCs). COPD and CF lungs acted as controls. The number of PMCs per 100 nucleated cells and per photomicrograph was estimated along with the Ashcroft score of fibrosis. Mouse PMCs expressing green fluorescent protein (GFP), and those labeled with nanoparticles, were injected into the pleural space of mice given intranasal TGFβ1. Mouse lungs were lavaged and examined for the presence of GFP, α-smooth muscle actin (αSMA), and calretinin.

RESULTS: Calretinin-positive PMCs were found throughout IPF lungs, but not in COPD or CF. The number of PMCs correlated with the Ashcroft score. In mice, nanoparticle-laden PMCs were recoverable by bronchoalveolar lavage, depending on TGFβ1 dose. Fluorescent staining showed αSMA expression in GFP-expressing PMCs, with colocalization of GFP and αSMA.

CONCLUSIONS: PMCs can traffic through the lung and show myofibroblast phenotypic markers. PMCs are present in IPF lungs, and their number correlates with IPF severity. Since IPF presumably begins subpleurally, PMCs could play a pathogenetic role via mesothelial-mesenchymal transition.

Key Words: epithelial-mesenchymal transition, mesothelial-mesenchymal transition, idiopathic pulmonary fibrosis, pleural mesothelial cells, pathogenesis, cell trafficking

INTRODUCTION

Idiopathic pulmonary fibrosis (IPF) is a progressive lung disease characterized by cellular and structural changes in the parenchyma caused by proliferating myofibroblasts. For reasons that are not well understood, this process is thought to begin in the subpleural region, and then extend centrally. Proliferating myofibroblasts expressing α-smooth muscle actin (αSMA) are thought to be the key cells responsible for the pathologic changes of IPF characterized by increased deposition of extracellular matrix components including collagen [1-3]. Neither the origin of these myofibroblasts nor the molecular mechanisms involved in their formation in the fibroblastic foci are clearly understood. A variety of sources have been postulated as origins for these myofibroblasts including circulating progenitor cells [4] and resident mesenchymal cells [1, 4].

It is currently believed that the fibroblasts are derived in part from local tissues following the process of epithelial-mesenchymal transition (EMT) [5]. We have recently demonstrated *in vitro* that pleural mesothelial cells (PMCs) have the capacity to transition into a myofibroblast phenotype and undergo haptotactic migration in response to transforming growth factor β1 (TGFβ1) [6]. We therefore hypothesized that such a process could also occur *in vivo*, leading to the characteristic findings seen on histopathology of IPF. This process can be denominated as "mesothelial-mesenchymal transition," a specialized form of EMT.

The pleural mesothelium is a metabolically active monolayer of cells that blankets the chest wall and lungs in parietal and visceral covers. During parenchymal inflammation the PMCs are exposed to a microenvironment with high levels of cytokines, chemokines and growth factors including TGFβ1 [7-9]. TGFβ1 is considered to be a master switch for the induction of fibrosis by a process of EMT in various organs including the lung [10-13]. With stress or injury, PMCs attain plasticity, losing their polarity and mesothelial markers. The cellular transition of PMCs leads to cytoskeletal reorganization, acquiring a spindle shape and expressing mesenchymal markers. The transformed PMCs lose the expression of adherens junctional proteins E-cadherin and N-cadherin, as well as cytokeratin.

Because of its intimate proximity to the lung parenchyma, the pleura can respond to inflammatory cytokines released by exogenous inhaled agents in animals [14] as well as humans [15]. Thus IPF may be a disease where inhaled mediators cause parenchymal release of cytokines such as TGFβ1, leading to mesothelial activation, EMT, and subsequent haptotaxis of activated myofibroblasts that form a cascading network of fibrosis starting at the subpleural region and invaginating towards the hilum [16, 17].

Indeed, a recent study has shown that hallmark lesion of IPF, the fibroblastic focus, is not a discrete site of epithelial injury and repair [18]. Instead, the fibroblastic foci seen on two-dimensional histopathological sections are part of a complex and highly interconnected reticulum of polyclonal fibrous tissue that is reactive rather than malignant. Three-dimensional reconstruction showed that the leading edge of this invasion extends from the pleura to the underlying parenchyma.

Interestingly, in a mouse model of intrapleural bleomycin and carbon black co-administration, pleural fibrosis was demonstrated extending into the parenchyma [19]. The subpleural distribution of fibrosis recapitulated the histopathology of IPF. Carbon particles were thought to be the "second hit," similar to cigarette smoke that can predispose patients to IPF in the appropriate phenotype [20].

All of these findings suggest that the pleural EMT can be a source of fibroblastic proliferation that invades the lung in IPF. Therefore, in our study we hypothesized that PMCs traffic through IPF lungs while undergoing EMT leading to fibrosis. We also hypothesized that key elements of

this paradigm that are difficult to study in human tissues can be recapitulated in a TGFβ1 mouse model of pulmonary fibrosis, further validating our proposed pathogenetic mechanism.

Materials and methods

Explanted IPF lungs: After informed consent, lungs of patients with IPF, chronic obstructive pulmonary disease (COPD), cystic fibrosis (CF), and idiopathic pulmonary arterial hypertension were preserved following lung transplantation at Inova Fairfax Hospital (Falls Church, VA) and Shands Hospital at University of Florida (Gainesville, FL). One patient who underwent a pneumonectomy for hemorrhage from a broncholith was also included as a control. The specimens were fixed in formalin, embedded in paraffin, and sectioned with a microtome before immunohistochemical staining on standard microscope slides. All biopsies were taken from the lower lobes and included the pleura and subjacent tissue.

Immunohistochemistry for calretinin and mesothelin in human lungs: Explanted lung slides were incubated with an antibody to calretinin (Cell Marque, Rocklin, CA) and mesothelin (Invitrogen, Carlsbad, CA) at a concentration of 1:500 and 1:100 respectively for 30 minutes at room temperature before washing and incubation with a secondary biotinylated anti-mouse IgG antibody (Vector Labs, Burlingame, CA) for 30 minutes at room temperature. Color was developed using VectaStain/kit (Vector Labs, Burlingame, CA) with VIP substrate for magenta/pink color and diaminobenzidine (DAB) for brown color. A light green counterstain was used to enhance the parenchyma with VIP and hematoxylin was used as a counterstain with DAB. The slides were visualized at 400X magnification. Any slides where the pleura did not

stain strongly for calretinin were rejected as inadequately stained and a new slide from the same tissue was restained. Fluorescence microscopy was also performed with these two antibodies using Texas Red and fluorescein isothiocyanate (green) labeled secondary antibodies staining as described in the fluorescent microscopy section below.

Calretinin-positive cellular counts: Two observers visualized each slide from explanted IPF lungs. The pleura was identified first so that adequacy of calretinin staining could be confirmed. Five photomicrographs were then randomly taken and the number of calretinin-positive cells per photomicrograph as well as the total number of nucleated cells were recorded.

Ashcroft score: For all IPF lungs, the Ashcroft fibrosis score [21] was assigned for each photomicrograph where calretinin-positive cells were counted. As with calretinin-positive cells, two observers determined the Ashcroft score.

Clinical data: After IRB approval, demographic data, pulmonary function tests, and details of clinical course IPF, COPD, and CF patients were extracted from the electronic medical records at Inova Fairfax Hospital and Shands Hospital at University of Florida.

GFP-positive mouse mesothelial cells: After approval from the institutional animal care committee, lungs of C57BL/6J mice (Jackson Laboratories, Bar Harbor, ME) that constitutively express green fluorescent protein (GFP) were harvested following euthanasia. The mesothelial cells were extracted by trypsinization as we have previously described [22] and resuspended in culture using Media-199 (Gibco Laboratories, Grand Island, NY) containing 10% FBS (Atlanta

Biologicals, Lawrenceville, GA), and penicillin (100 Units/ml) with streptomycin (100 μg/ml) (Cellgro, Mediatech, Herndon, VA). The cells were plated in 75 cm^2 culture flasks (Corning Costar Corporation, MA) and incubated at 37° C in 5% CO_2 and 95% air. The medium was changed on alternate days, or as needed.

Mouse mesothelial cell culture: Mouse mesothelial cell in primary culture were plated in 75 cm^2 culture flasks with F12K (Gibco Laboratories, Grand Island, NY) supplemented with 10% heat-inactivated FBS, penicillin (100 U/mL), and streptomycin (100 μg/mL), 1% amphotericin B (Gibco), 1 mM sodium pyruvate (Gibco), and 10 mM HEPES buffer (Sigma-Aldrich, St. Louis, MO). Cells were maintained at 37° C in a humidified atmosphere with 95% air and 5% CO_2. The medium was changed on alternate days or as needed.

Labeling mouse mesothelial cells with nanoparticles: Mesothelial cells (1 x 10^6) from C57BL/6J mice were plated in 60-mm dishes with serum free F12K medium. Cells were incubated with silica nanoparticles coated with tetramethyl rhodamine isothiocyanate (TRITC) dye at 37° C in a humidified atmosphere with 95% air and 5% CO_2 for 24 hours. Silica nanoparticles are nontoxic to cultured cells [23, 24]. After the incubation, cells were washed and centrifuged for 5 minutes at 1500 rpm, the pellet was resuspended in 200 μL of phosphate buffered-saline (PBS) to remove any free nanoparticles, and injected into the pleural space of the mice using an Angiocath (Becton Dickinson, Franklin Lakes, NJ) as previously described [25].

TGFβ1 mouse model: Labeled or GFP-positive mouse mesothelial cells were injected into the pleural space of C57BL6J mice (Jackson Laboratories, Bar Harbor, ME) using our previously

described techniques [22]. Accidental injection into lung parenchyma leads to bilateral pneumothorax and death since the mouse has only one pleural cavity. TGFβ1 (PeproTech, Rocky Hill, NJ) was nasally delivered to the lungs at varying doses. Lungs were harvested after euthanasia at different time points. The lungs were carefully examined and no injection injury was found in any lung.

Mouse bronchoalveolar lavage, serum collection and tissue harvest: Bronchoalveolar lavage (BAL) was performed at different time points after intrapleural injection of TRITC-laden PMCs into mice given intranasal TGFβ1 or saline. Fluid was collected by injecting 800-1000 μL Hank's balanced salt solution into the lungs via tracheal cannulation. The fluid was aspirated and the process was repeated for a total of 1600-2000 μL of BAL fluid collected. BAL fluid was centrifuged at 1500 rpm for 5 minutes to pellet the cells and separate the supernatant. BAL cells were analyzed for fluorescence by reading the optical density at 541 nm to detect the nanoparticles. The lungs were then perfused via the pulmonary artery with HBSS to clear the red blood cells. Optimal Cutting Temperature (OCT) compound (800 μL) was injected into the lungs via tracheal cannulation to preserve lung architecture. Lungs were harvested and stored in OCT for frozen section analysis.

Fluorescent microscopy: Frozen mouse lung tissue sections were fixed with 4% paraformaldehyde for 10 minutes at room temperature, after washing with PBS twice. The slides were incubated with anti-αSMA rabbit anti-mouse antibody (Biocare, Concord, CA) for 1 h and Texas Red goat anti-rabbit antibody (Invitrogen, Carlsbad, CA) for 30 min. The nuclei were stained for DAPI (Molecular Probes, Eugene, OR) for 10 minutes in the dark. The sections were

then washed with PBS twice and the cover slide was mounted with SlowFade Antifade kit (Molecular Probes, Eugene, OR). The GFP and Texas Red signal was analyzed in each tissue using a specific filter using a fluorescent microscope (Zeiss LSM 510 Axiovert 200M, Zeiss, Thornwood, NY).

Statistical analysis: The data analyses were performed by using Excel 12.2 software (Microsoft, Redmond, WA).

RESULTS

Demographic characteristics of the study group.

Twenty-eight patients were included in the study. The age ranged from 8 to 71. All of the patients underwent lung transplantation between 2006 and 2009. Sixteen patients were diagnosed with IPF, 8 patients with COPD, 2 patients with CF, and 1 with IPAH. Tissue from one patient who suffered from severe hemorrhage due to a broncholith and required a pneumonectomy was also included. The diagnosis was made based upon generally accepted criteria for each disease. Table 1 shows the characteristics of the human subjects included in this study.

Calretinin positive cells correlate with the degree of fibrosis in human lung tissue.

We stained IPF human lung sections for calretinin and obtained 5 photomicrographs for each specimen. The calretinin-positive cells were found predominantly in the areas of interstitial fibrosis. Rarely, they could also be seen in and around bronchioli. Two observers estimated the Ashcroft score of the degree of fibrosis, the number of calretinin-positive cells, and the total number of nucleated cells in each photomicrograph. In case there was minor disagreement between the two observers, the Ashcroft score and/or the number of calretinin positive cells were averaged. If the disagreement in the number of calretinin-positive cells was more than 15%, the cells were counted again. Altogether, each observer counted more than 40,000 nucleated cells.

We found a significant positive correlation between the number of calretinin stained cells and the degree of fibrosis in a given photomicrograph (Fig. 1A). We also found that the number of calretinin-positive cells per 100 nucleated cells correlated with the Ashcroft score for that patient (Fig. 1B).

Immunohistochemistry for calretinin in human lung tissue.

Figure 2 shows the positive calretinin staining of mesothelial cells in the fibrotic lungs from patients with IPF. The pleura stained intensely (pink) indicating the presence of calretinin (Panel A). When the parenchyma was stained, calretinin-positive cells were found throughout the parenchyma (Panel B). When the lung samples from patients with COPD were analyzed, only rare calretinin-positive cells were noted in emphysematous lung. Similarly, only rare calretinin-positive cells were noted in CF, IPAH, and normal lung.

Immunohistochemistry for mesothelin in human lung tissue.

Calretinin is only 95% sensitive and 86% specific for cells of mesothelial origin [26]. To confirm that the cells detected by calretinin staining were of mesothelial origin, a second stain, mesothelin, was employed. Mesothelin is 73% sensitive and 55% specific for the mesothelium [26], but combined with calretinin, further increases the sensitivity and specificity for cells of pleural origin. Consecutive microtome sections were obtained through IPF lungs. Adjacent sections were stained with calretinin and mesothelin using exactly the same reagents, concentrations, and incubation times. The same cluster of cells that stains positively for calretinin (Figure 3A and 3C) also stains for mesothelin (Figure 3B and 3D).

Fluorescence microscopy for calretinin and mesothelin in human lung tissue

Figure 3E, F, G, and H show that lungs stained with IPF when stained for calretinin demonstrate positivity in the parenchyma (Texas Red). Furthermore, when the same section is stained for mesothelin (fluorescein isothiocyanate), the same cells show positivity for mesothelin. The

concordance of staining is not 100%, as would be expected from mesothelial markers that have different sensitivities and specificities for mesothelial origin.

Mouse mesothelial cells laden with TRITC nanoparticles were present in the BAL fluid of TGFβ1 treated mice.

Figure 4A shows the increase of fluorescence in a dose and time dependent manner in BAL from TGFβ1-treated mice as compared to saline control mice. The results represent the mean of 3 mice for each group. Figure 4B and C show fluorescence imaging of BAL fluid from TGFβ1 and saline treated mice. The BAL fluid from mice treated with 1.5 ng of TGFβ1 demonstrates nanoparticles at 24 hours while the fluid from saline control mice does not. Figure 4D, E, and F demonstrate fluorescence imaging of lung histopathology. The nanoparticles can be found inside the parenchyma with 1.5 ng of TGFβ1 at 12 hours (E), while none can be seen with saline (D). Even at 48 hours, the nanoparticles remain at the pleural surface with saline (F). Together, these data indicate the migration of these cells injected into the pleural space though the parenchyma under the influence of TGFβ1.

GFP-expressing mouse mesothelial cells migrate into the lung parenchyma in TGFβ1 treated mice.

To further confirm the results with nanoparticle-laden mesothelial cells found in the BAL in TGFβ1 inoculated mice, we repeated the same experiment but injected GFP-expressing mesothelial cells into the pleural space of TGFβ1 or saline pre-treated mice. Figure 5 shows a GFP-positive signal inside the lung parenchyma of mice treated with TGFβ1 as compared with saline inoculated mice. This indicated the migration of GFP-expressing mesothelial cells from

the pleural space to the parenchyma when mice were treated with TGFβ1. Furthermore, when stained with Texas Red for the presence of αSMA, the GFP-labeled cells demonstrate a yellow color, indicating that the GFP-labeled PMCs have now begun to express αSMA.

DISCUSSION

In this study, we demonstrate the presence of calretinin-positive cells in explanted lung tissue in IPF. This phenomenon appears to be specific to patients with IPF, since we observed only rare calretinin-positive cells in normal lung tissue, emphysematous lung tissue, and cystic fibrosis lung tissue. Just as leukocytes gravitate to areas of infection and inflammation via chemotaxis, these PMCs appear to be attracted to areas of fibrosis.

We were able to demonstrate a correlation between the number of calretinin-positive cells and the degree of fibrotic change in the parenchyma, as measured by the Ashcroft score. Whether the number of calretinin-positive cells was measured as a raw number, or as percentage of the total nucleated cells seen in a photomicrograph, the correlation with the degree of fibrosis was highly significant. The Ashcroft score was originally described in 1988, but over more than 20 years, it remains the best and time-honored score for histopathological grading of pulmonary fibrosis [27-32]. The scale starts at 0 that indicates normal lung. A score of 1 represents minimal fibrosis, 3 represents minimal fibrosis with preserved architecture, 5 indicates definite distortion with fibrous bands, 7 denotes severe distortion with honeycomb change, while 8 connotes total fibrous obliteration.

The fact that these cells could have originated from the pleural surface invading the lung parenchyma is borne out by our TGFβ1 mouse model. This process is dose- as well as time-dependent. Whether one looks at PMCs labeled with GFP or nanoparticles, these cells invade

the lung parenchyma in response to TGFβ1, a well-known growth factor that induces fibrosis in murine models.

This work is a follow up study to our recent paper showing haptotactic migration of PMCs *in vitro* [6]. When cultured PMCs were exposed to a profibrotic stimulus like TGFβ1 they underwent EMT in a smad2-dependent manner. The phenotype of these cells changed to a fibroblastic morphology with simultaneous expression of αSMA, fibroblast specific protein-1, and collagen type I. This transition was accompanied by migration of these cells along the TGFβ1 gradient.

There are important differences between the murine and human pleura. The mesothelial layer in mice lies in close proximity to the parenchyma, but in humans it has subjacent vasculature and stroma. Thus mesothelial trafficking in the human condition needs to overcome more anatomical barriers than the murine situation. Therefore extrapolation of results from the mouse to human must be done with caution.

Traditionally, PMCs have been thought to remain relatively quiescent on the apposing surfaces of the lung and chest wall. Their primary purpose has been thought to be production of a lubricating layer of pleural fluid to facilitate expansion of the lung by reducing friction with the encasing musculoskeletal structures of the thorax. Their role in host defense and fighting infections such as empyema has also been well recognized [33]. However, despite the proximity to the pulmonary parenchyma and despite subpleural patterns seen in several lung diseases, the pleura has been thought to be an innocent bystander in parenchymal disease. Pleural plaques

from asbestos lung disease and empyema from parenchymal infections have been congruent with this notion that the parenchyma can affect the pleura, but not vice versa. Our study supports the notion that the reverse may also hold true. Therefore we speculate that in IPF this metabolically active layer of cells may be more pathophysiologically important than previously thought.

IPF is also characterized by basal predominance. However, there is increasing evidence that when the apicobasal gradient is absent, genetic mutations may be responsible [34-36]. Our study did not study this phenomenon since all the biopsy specimens were taken from the lower lobes, nor did we attempt to look for such mutations.

Interestingly, there have been hints in the literature that mesothelial cells are not stationary, and far more responsive to the local microenvironment than once believed. PMCs can traffic through the lung parenchyma and appear in mediastinal lymph nodes [37]. Mesothelioma can be misdiagnosed as metastatic when in fact it is localized [38]. A similar process has been noted in the peritoneum. Ovarian carcinoma can be misdiagnosed as metastatic because of the presence of peritoneal mesothelial cells in pelvic lymph nodes [39-41]. Therefore it is quite likely that PMCs traffic through the lungs under pathological conditions, and perhaps at a slower rate even in physiological conditions.

Our work builds upon the seminal work of Decologne and colleagues [42] who have demonstrated congruent findings in a different model of fibrosis. While our model has used inhaled TGFβ1, Decologne used adenovirally mediated transient TGFβ1 expression in the pleural mesothelium leading to pleural fibrosis but no pleurodesis. There was subpleural fibrosis

in the parenchyma via EMT, but none in the chest wall. Since we believe that an inhaled stimulus is more likely to cause IPF than a pleural infection, we chose to deliver TGFβ1 via inhalation in our model and correlate that with histopathology of human IPF. However, our model has an important limitation in that it is a short-term model that is unable to quantify the development of fibrosis, such as using hydroxyproline.

Recent evidence has shown that the pleural surface reacts to inhaled antigens very quickly. Inhaled ovalbumin produces pleural edema detectable by MRI and histopathology within 3 hours. Thus it is quite possible that environmental agents can provoke a cascade of pleural inflammation that initiates a wave of fibrosis caused by trafficking PMCs that undergo EMT as they transform normal parenchyma into honeycomb lung in a centripetal fashion.

Pulmonary fibrosis caused by asbestos may share certain similarities with the foregoing hypothesis. Asbestos lung disease can manifest decades after the original exposure, with the particles slowly migrating from the parenchyma to the pleura [43]. In many instances, the fibers may no longer be detectable, presumably being catabolized by macrophages or tissue enzymes [44]. However, even in such cases, the changes brought about by asbestos can eventually lead to mesothelioma, presumably by chronic parenchymal activation or inflammation. Therefore the pleura and the parenchyma can interact to produce pathology in multiple lung conditions, and IPF may be only one such clinical paradigm.

Our findings raise the question as to whether or not dysregulated PMCs can cause IPF? It does appear that our data meet at least some of the criteria for causality [45]. These include the finding

that the presence of mesothelial cells in lung parenchyma is relatively *specific* to IPF, and does not seem to occur in COPD or CF. We counted a higher number of PMCs in areas that had higher grade of fibrosis. Moreover, the PMCs made up a higher percentage of cells in areas with higher grade of fibrosis. Thus the *strength of association* between the geographic heterogeneity of fibrosis and the number of mesothelial cells suggests that a *dose-response relationship* could exist. This is further supported by the *dose-response relationship* in our mouse models of TGFβ1 and pulmonary fibrosis. Given the findings of EMT in mesothelial cells *in vitro*, it appears *biologically plausible* that mesothelial cells could transition into myofibroblasts *in vivo*.

Although it is possible, and indeed likely, that other cell lineages contribute to fibrosis via EMT, the notion that pleural EMT may cause or contribute to fibrosis is *reasoned and consistent* with the natural history and biology of the disease. Specifically, the disease is known to start subpleurally, and progress into the parenchyma suggesting a centripetal invading wave of fibrosis that is accompanied by clinical worsening. Further supportive experimental evidence will be required including the use of selective knock-in mice that permanently mark adult cell lineages such as PMCs. Nonetheless, our findings provide preliminary evidence that the pleural surface may not be an innocent bystander in the pathogenesis of this deadly disease.

REFERENCES

1. Kalluri R, Neilson EG. Epithelial-mesenchymal transition and its implications for fibrosis. *J Clin Invest* 2003: 112(12): 1776-1784.

2. Neilson EG, Plieth D, Venkov C. Epithelial-mesenchymal transitions and the intersecting cell fate of fibroblasts and metastatic cancer cells. *Transactions of the American Clinical and Climatological Association* 2003: 114: 87-100; discussion 100-101.

3. Noble PW. Idiopathic pulmonary fibrosis. New insights into classification and pathogenesis usher in a new era therapeutic approaches. *Am J Respir Cell Mol Biol* 2003: 29(3 Suppl): S27-31.

4. Abe R, Donnelly SC, Peng T, Bucala R, Metz CN. Peripheral blood fibrocytes: differentiation pathway and migration to wound sites. *J Immunol* 2001: 166(12): 7556-7562.

5. Iwano M, Plieth D, Danoff TM, Xue C, Okada H, Neilson EG. Evidence that fibroblasts derive from epithelium during tissue fibrosis. *J Clin Invest* 2002: 110(3): 341-350.

6. Nasreen N, Mohammed KA, Mubarak KK, Baz MA, Akindipe OA, Fernandez-Bussy S, Antony VB. Pleural mesothelial cell transformation into myofibroblasts and haptotactic migration in response to TGF-{beta}1 in vitro. *Am J Physiol Lung Cell Mol Physiol* 2009: 297(1): L115-124.

7. Strutz F, Zeisberg M, Ziyadeh FN, Yang CQ, Kalluri R, Muller GA, Neilson EG. Role of basic fibroblast growth factor-2 in epithelial-mesenchymal transformation. *Kidney international* 2002: 61(5): 1714-1728.

8. Pochetuhen K, Luzina IG, Lockatell V, Choi J, Todd NW, Atamas SP. Complex Regulation of Pulmonary Inflammation and Fibrosis by CCL18. *Am J Pathol* 2007.

9. Broekelmann TJ, Limper AH, Colby TV, McDonald JA. Transforming growth factor beta 1 is present at sites of extracellular matrix gene expression in human pulmonary fibrosis. *Proc Natl Acad Sci U S A* 1991: 88(15): 6642-6646.

10. Willis BC, duBois RM, Borok Z. Epithelial origin of myofibroblasts during fibrosis in the lung. *Proceedings of the American Thoracic Society* 2006: 3(4): 377-382.

11. Zeisberg M, Kalluri R. The role of epithelial-to-mesenchymal transition in renal fibrosis. *J Mol Med* 2004: 82(3): 175-181.

12. Friedman SL. Molecular regulation of hepatic fibrosis, an integrated cellular response to tissue injury. *J Biol Chem* 2000: 275(4): 2247-2250.

13. Verrecchia F, Mauviel A. Transforming growth factor-beta and fibrosis. *World J Gastroenterol* 2007: 13(22): 3056-3062.

14. Quintana HK, Cannet C, Schaeublin E, Zurbruegg S, Sugar R, Mazzoni L, Page CP, Fozard JR, Beckmann N. Identification with MRI of the pleura as a major site of the acute inflammatory effects induced by ovalbumin and endotoxin challenge in the airways of the rat. *Am J Physiol Lung Cell Mol Physiol* 2006: 291(4): L651-657.

15. Song Y, Li X, Du X. Exposure to nanoparticles is related to pleural effusion, pulmonary fibrosis and granuloma. *Eur Respir J* 2009: 34(3): 559-567.

16. Antony VB. Immunological mechanisms in pleural disease. *Eur Respir J* 2003: 21(3): 539-544.

17. Quintana HK, Cannet C, Schaeublin E, Zurbruegg S, Sugar R, Mazzoni L, Page CP, Fozard JR, Beckmann N. Identification with MRI of the pleura as a major site of the acute inflammatory effects induced by ovalbumin and endotoxin challenge in the airways of the rat. *Am J Physiol Lung Cell Mol Physiol* 2006: 291(4): L651-657.

18. Cool CD, Groshong SD, Rai PR, Henson PM, Stewart JS, Brown KK. Fibroblast Foci Are Not Discrete Sites of Lung Injury or Repair: The Fibroblast Reticulum. *Am J Respir Crit Care Med* 2006: 174(6): 654-658.

19. Decologne N, Wettstein G, Kolb M, Margetts P, Garrido C, Camus P, Bonniaud P. Bleomycin induces pleural and subpleural fibrosis in the presence of carbon particles. *Eur Respir J* 2009: 09031936.00181808.

20. Baumgartner KB, Samet JM, Stidley CA, Colby TV, Waldron JA. Cigarette smoking: a risk factor for idiopathic pulmonary fibrosis. *Am J Respir Crit Care Med* 1997: 155(1): 242-248.

21. Ashcroft T, Simpson JM, Timbrell V. Simple method of estimating severity of pulmonary fibrosis on a numerical scale. *J Clin Pathol* 1988: 41(4): 467-470.

22. Mohammed KA, Nasreen N, Ward MJ, Antony VB. Helper T cell type 1 and 2 cytokines regulate C-C chemokine expression in mouse pleural mesothelial cells. *Am J Respir Crit Care Med* 1999: 159(5 Pt 1): 1653-1659.

23. Faisal M, Hong Y, Liu J, Yu Y, Lam JW, Qin A, Lu P, Tang BZ. Fabrication of fluorescent silica nanoparticles hybridized with AIE luminogens and exploration of their applications as nanobiosensors in intracellular imaging. *Chemistry* 2010: 16(14): 4266-4272.

24. Yang H, Wu Q, Tang M, Liu X, Deng H, Kong L, Lu Z. In vitro study of silica nanoparticle-induced cytotoxicity based on real-time cell electronic sensing system. *J Nanosci Nanotechnol* 2010: 10(1): 561-568.

25. Mohammed KA, Nasreen N, Ward MJ, Antony VB. Induction of acute pleural inflammation by Staphylococcus aureus. I. CD4+ T cells play a critical role in experimental empyema. *J Infect Dis* 2000: 181(5): 1693-1699.

26. Kachali C, Eltoum I, Horton D, Chhieng DC. Use of mesothelin as a marker for mesothelial cells in cytologic specimens. *Semin Diagn Pathol* 2006: 23(1): 20-24.

27. Hagiwara SI, Ishii Y, Kitamura S. Aerosolized administration of N-acetylcysteine attenuates lung fibrosis induced by bleomycin in mice. *Am J Respir Crit Care Med* 2000: 162(1): 225-231.

28. Matsuoka H, Arai T, Mori M, Goya S, Kida H, Morishita H, Fujiwara H, Tachibana I, Osaki T, Hayashi S. A p38 MAPK inhibitor, FR-167653, ameliorates murine bleomycin-induced pulmonary fibrosis. *Am J Physiol Lung Cell Mol Physiol* 2002: 283(1): L103-112.

29. Simler NR, Howell DC, Marshall RP, Goldsack NR, Hasleton PS, Laurent GJ, Chambers RC, Egan JJ. The rapamycin analogue SDZ RAD attenuates bleomycin-induced pulmonary fibrosis in rats. *Eur Respir J* 2002: 19(6): 1124-1127.

30. Murakami S, Nagaya N, Itoh T, Kataoka M, Iwase T, Horio T, Miyahara Y, Sakai Y, Kangawa K, Kimura H. Prostacyclin agonist with thromboxane synthase inhibitory activity (ONO-1301) attenuates bleomycin-induced pulmonary fibrosis in mice. *Am J Physiol Lung Cell Mol Physiol* 2006: 290(1): L59-65.

31. Murakami S, Nagaya N, Itoh T, Fujii T, Iwase T, Hamada K, Kimura H, Kangawa K. C-type natriuretic peptide attenuates bleomycin-induced pulmonary fibrosis in mice. *Am J Physiol Lung Cell Mol Physiol* 2004: 287(6): L1172-1177.

32. Izumo T, Kondo M, Nagai A. Cysteinyl-leukotriene 1 receptor antagonist attenuates bleomycin-induced pulmonary fibrosis in mice. *Life Sci* 2007: 80(20): 1882-1886.

33. Jantz MA, Antony VB. Pathophysiology of the pleura. *Respiration* 2008: 75(2): 121-133.

34. Lawson WE, Crossno PF, Polosukhin VV, Roldan J, Cheng DS, Lane KB, Blackwell TR, Xu C, Markin C, Ware LB, Miller GG, Loyd JE, Blackwell TS. Endoplasmic reticulum stress in

alveolar epithelial cells is prominent in IPF: association with altered surfactant protein processing and herpesvirus infection. *Am J Physiol Lung Cell Mol Physiol* 2008: 294(6): L1119-1126.

35. Lawson WE, Grant SW, Ambrosini V, Womble KE, Dawson EP, Lane KB, Markin C, Renzoni E, Lympany P, Thomas AQ, Roldan J, Scott TA, Blackwell TS, Phillips JA, 3rd, Loyd JE, du Bois RM. Genetic mutations in surfactant protein C are a rare cause of sporadic cases of IPF. *Thorax* 2004: 59(11): 977-980.

36. Kottmann RM, Hogan CM, Phipps RP, Sime PJ. Determinants of initiation and progression of idiopathic pulmonary fibrosis. *Respirology* 2009: 14(7): 917-933.

37. Brooks JS, LiVolsi VA, Pietra GG. Mesothelial cell inclusions in mediastinal lymph nodes mimicking metastatic carcinoma. *Am J Clin Pathol* 1990: 93(6): 741-748.

38. Argani P, Rosai J. Hyperplastic mesothelial cells in lymph nodes: report of six cases of a benign process that can stimulate metastatic involvement by mesothelioma or carcinoma. *Hum Pathol* 1998: 29(4): 339-346.

39. Alvarado Cabrero I, Sosa Romero A. [Benign epithelial inclusions in pelvic lymph nodes. 2 case reports]. *Ginecol Obstet Mex* 2000: 68: 77-81.

40. Kir G, Eren S, Kir M. Hyperplastic mesothelial cells in pelvic and abdominal lymph node sinuses mimicking metastatic ovarian microinvasive serous borderline tumor. *Eur J Gynaecol Oncol* 2004: 25(2): 236-238.

41. Clement PB, Young RH, Oliva E, Sumner HW, Scully RE. Hyperplastic mesothelial cells within abdominal lymph nodes: mimic of metastatic ovarian carcinoma and serous borderline tumor--a report of two cases associated with ovarian neoplasms. *Mod Pathol* 1996: 9(9): 879-886.

42. Decologne N, Kolb M, Margetts PJ, Menetrier F, Artur Y, Garrido C, Gauldie J, Camus P, Bonniaud P. TGF-beta1 induces progressive pleural scarring and subpleural fibrosis. *J Immunol* 2007: 179(9): 6043-6051.

43. Beattie J, Knox JF. Studies of mineral content and particle size distribution in the lungs of asbestos textile workers. *In:* Davis CN, ed. Inhaled Particles and Vapours. Pergamon Press, London, 1961; pp. 419–432.

44. Nagelschmidt G. Some observations of the dust content and composition in lungs with asbestosis, made during work on coal miners pneumoconiosis. *Ann N Y Acad Sci* 1965: 132(1): 64-76.

45. Hill AB. The Environment and Disease: Association or Causation? *Proc R Soc Med* 1965: 58: 295-300.

Table 1: Demographics characteristics of the study population. The normal lung tissue was taken from a patient who suffered severe hemorrhage from a broncholith requiring a pneumonectomy. IPF = idiopathic pulmonary fibrosis. COPD = chronic obstructive pulmonary disease. CF = cystic fibrosis. IPAH = idiopathic pulmonary arterial hypertension.

Patients	Etiology	Mean Age	Percent Male
16	IPF	61	88%
8	COPD	58	38%
2	CF	23	50%
1	IPAH	8	0%
1	Normal	48	0%

Figure 1

A.

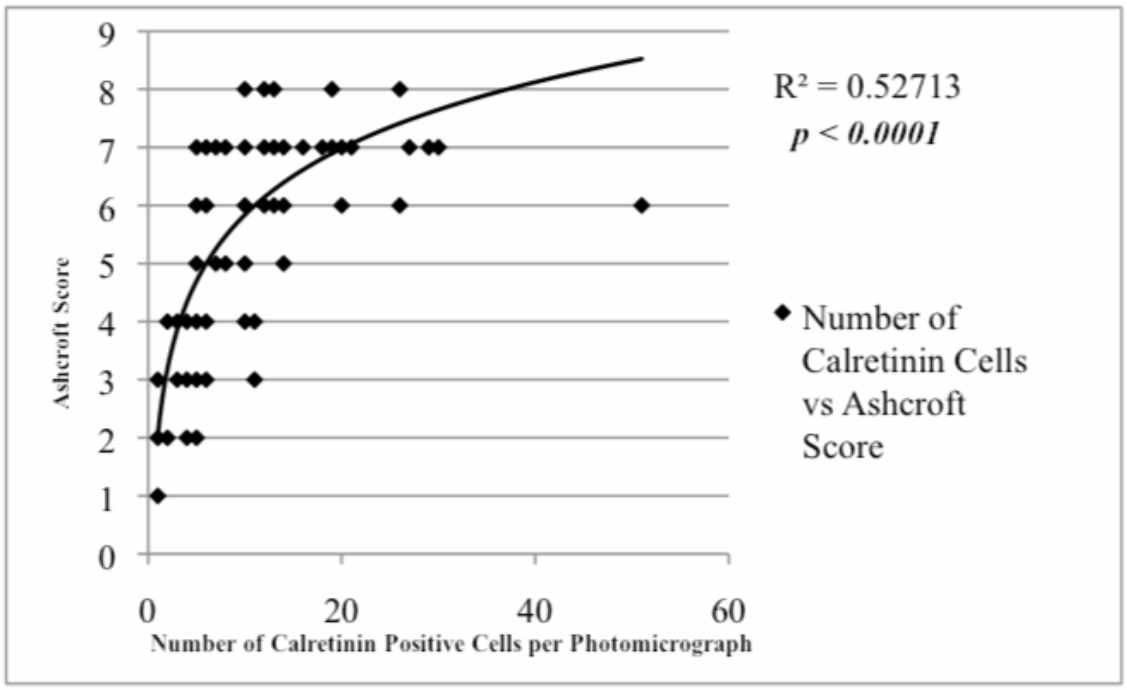
9
8
7
6
5
4
3
2
1
0
Ashcroft Score
0
20
40
60
Number of Calretinin Positive Cells per Photomicrograph
R² = 0.52713
p < 0.0001
Number of Calretinin Cells vs Ashcroft Score

B.

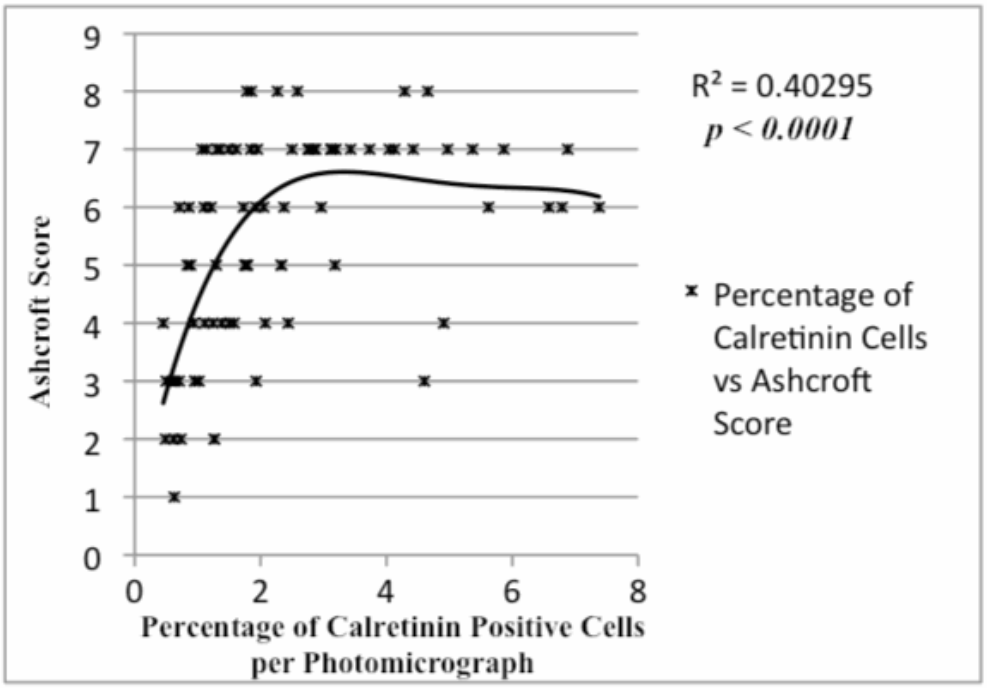
9
8
7
6
5
4
3
2
1
0
Ashcroft Score
0
2
4
6
8
Percentage of Calretinin Positive Cells per Photomicrograph
R² = 0.40295
p < 0.0001
Percentage of Calretinin Cells vs Ashcroft Score

Figure 2

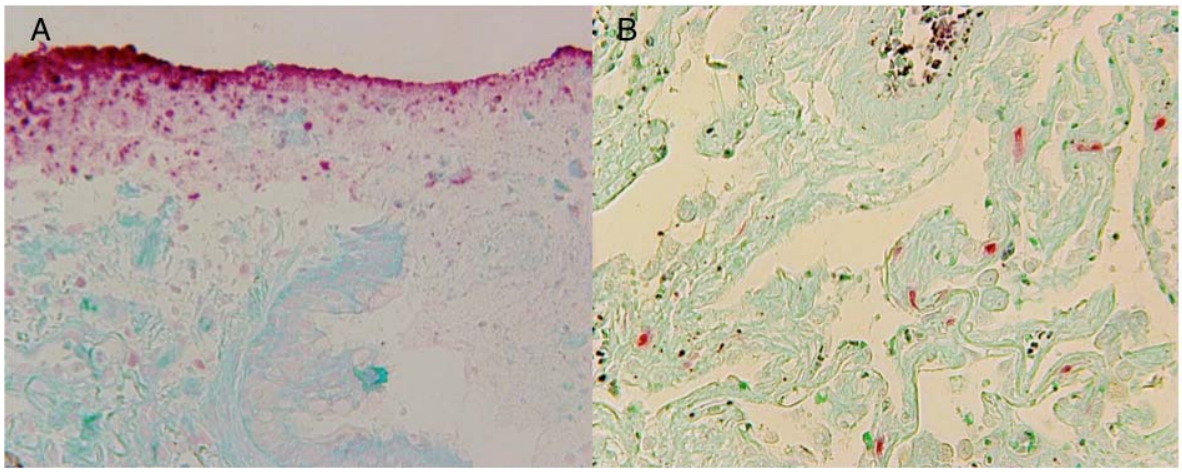

Figure 3

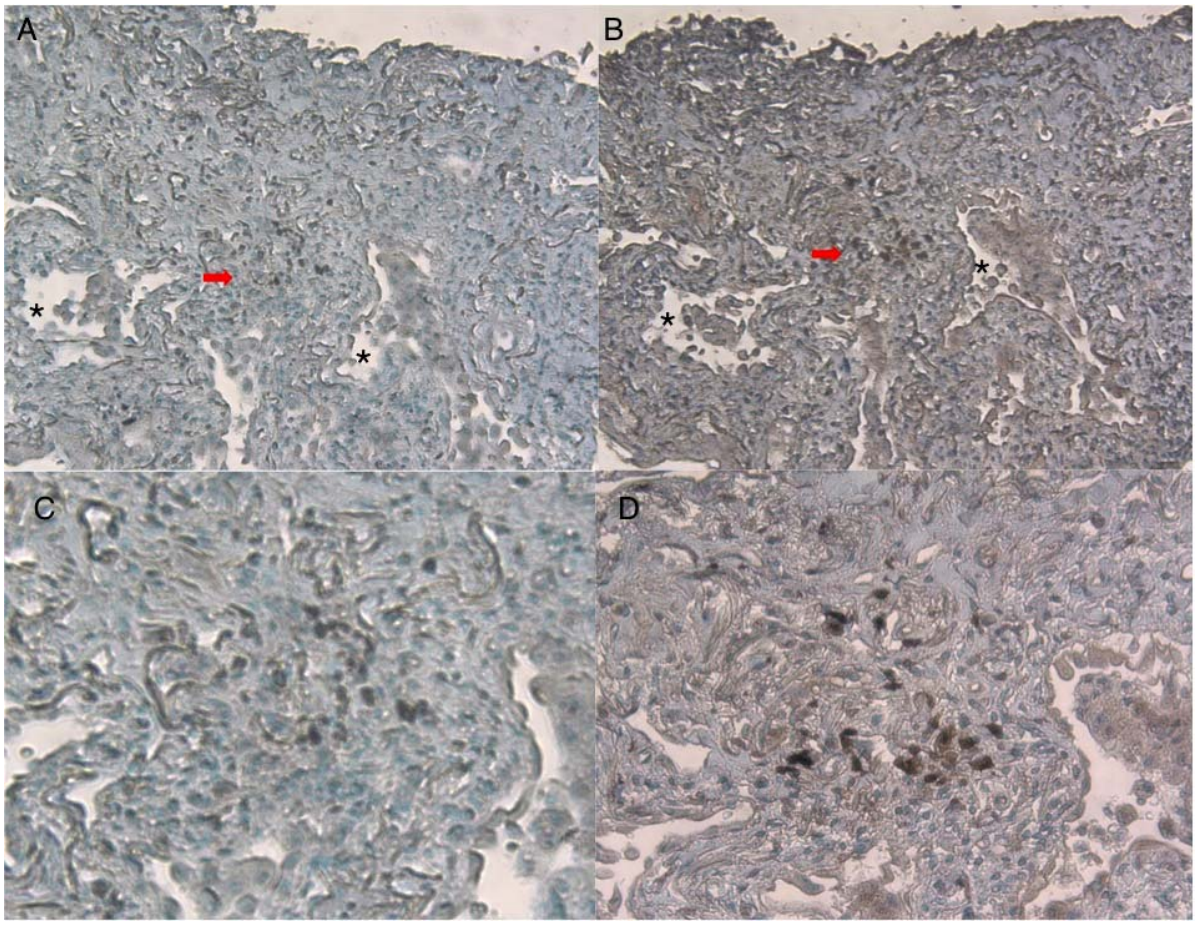

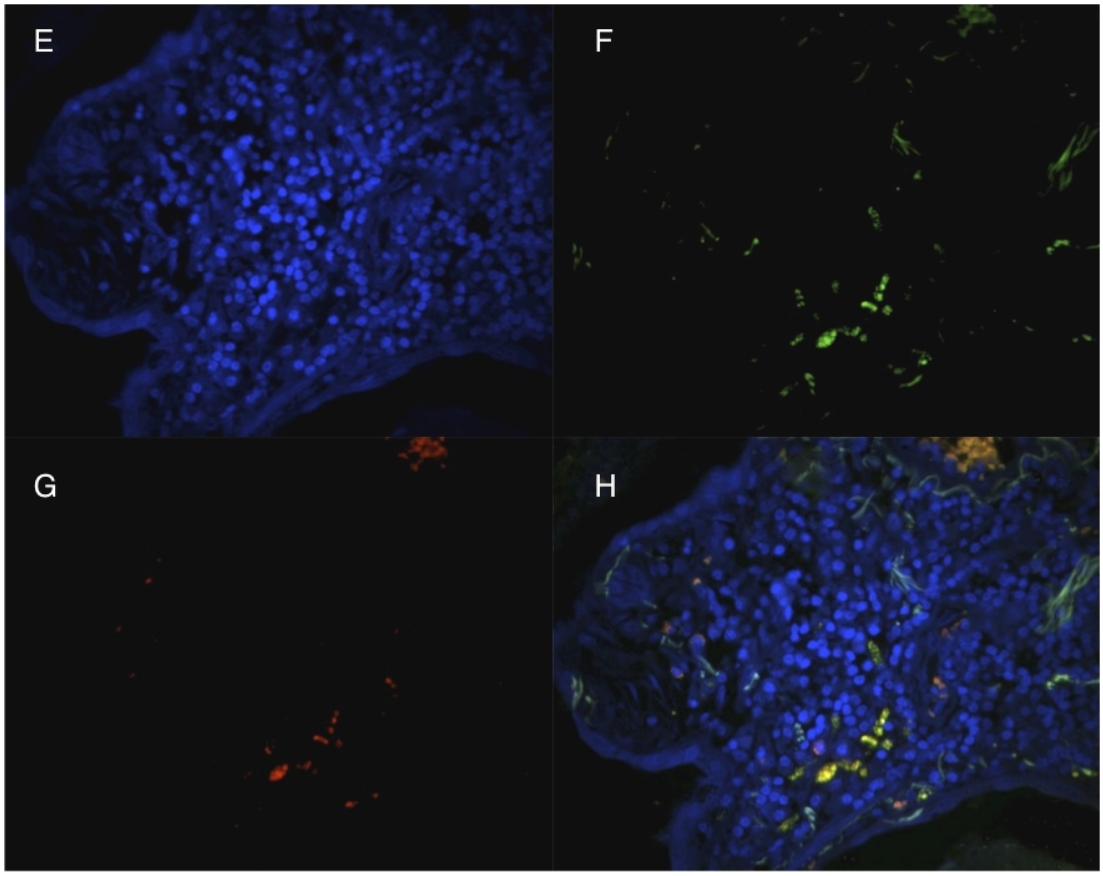

Figure 4

A.

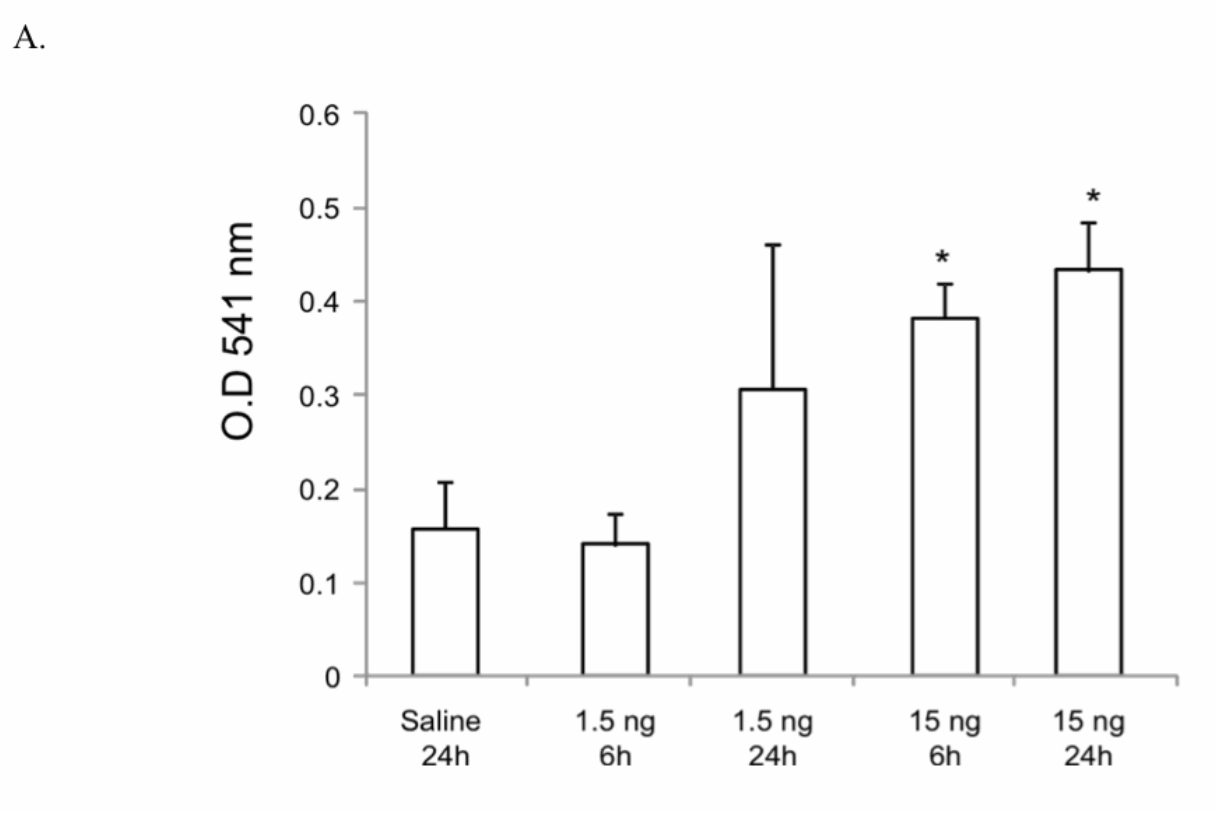
O.D 541 nm
0.6
0.5
0.4
0.3
0.2
0.1
0
*
*
Saline 24h
1.5 ng 6h
1.5 ng 24h
15 ng 6h
15 ng 24h

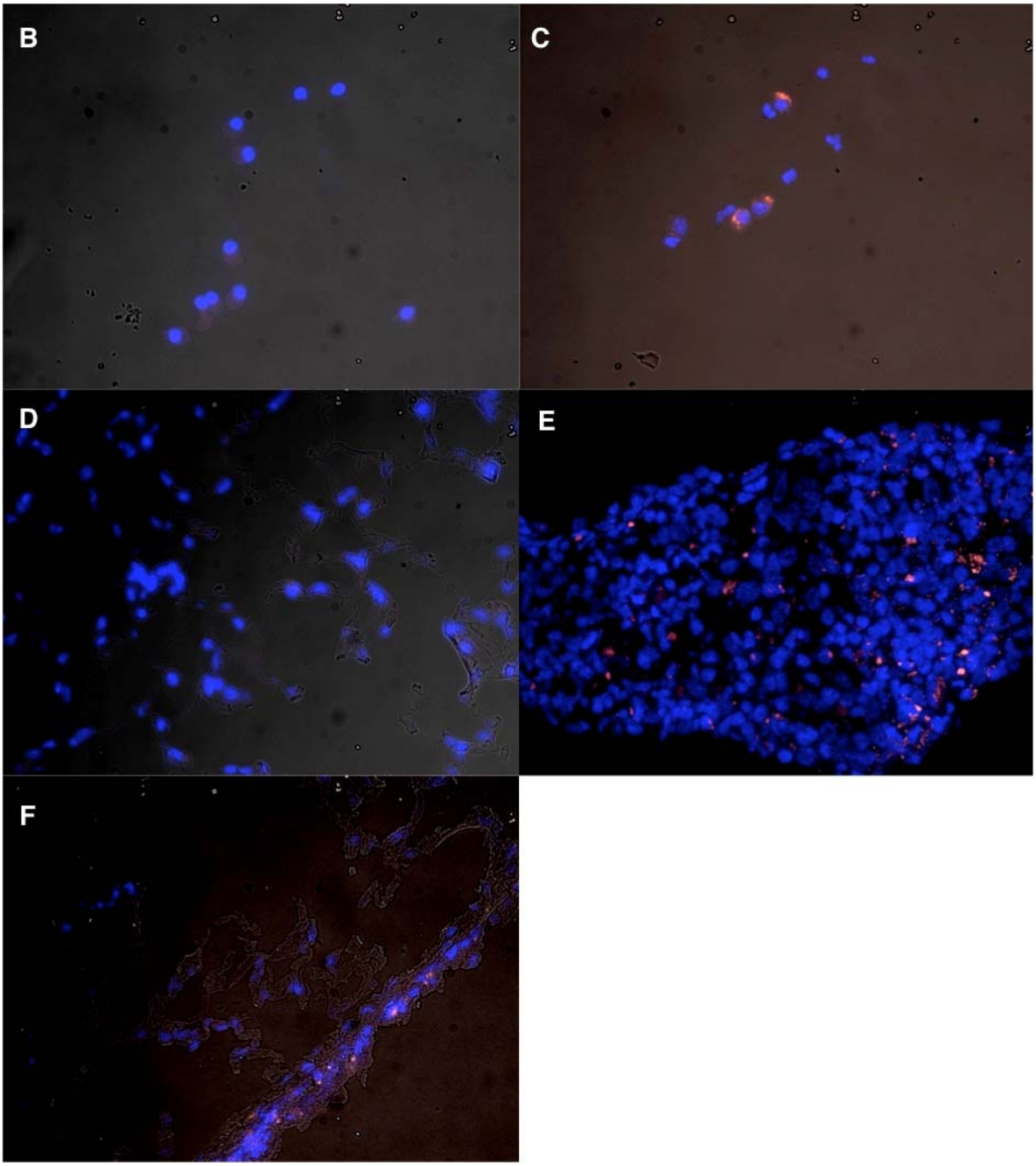
B
C
D
E
F

Figure 5

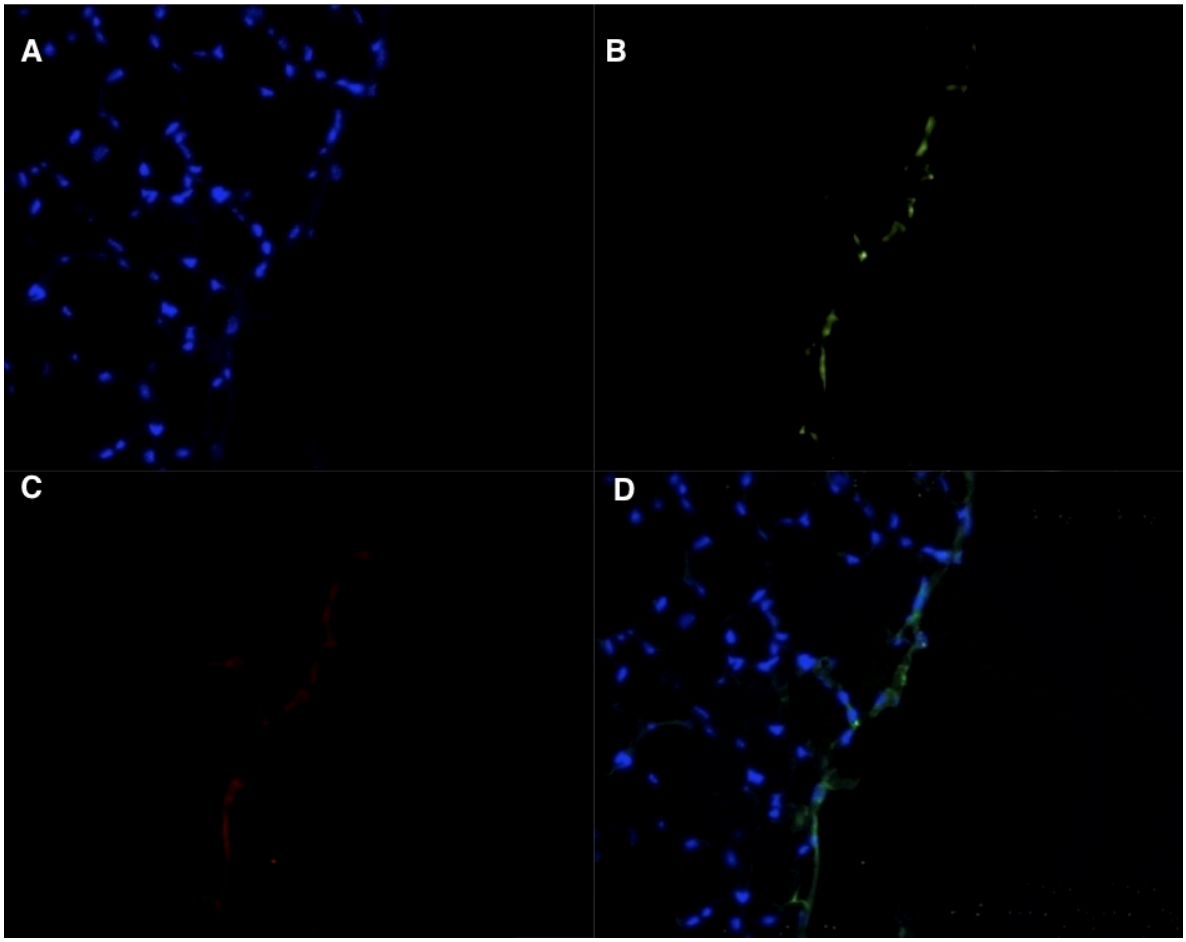

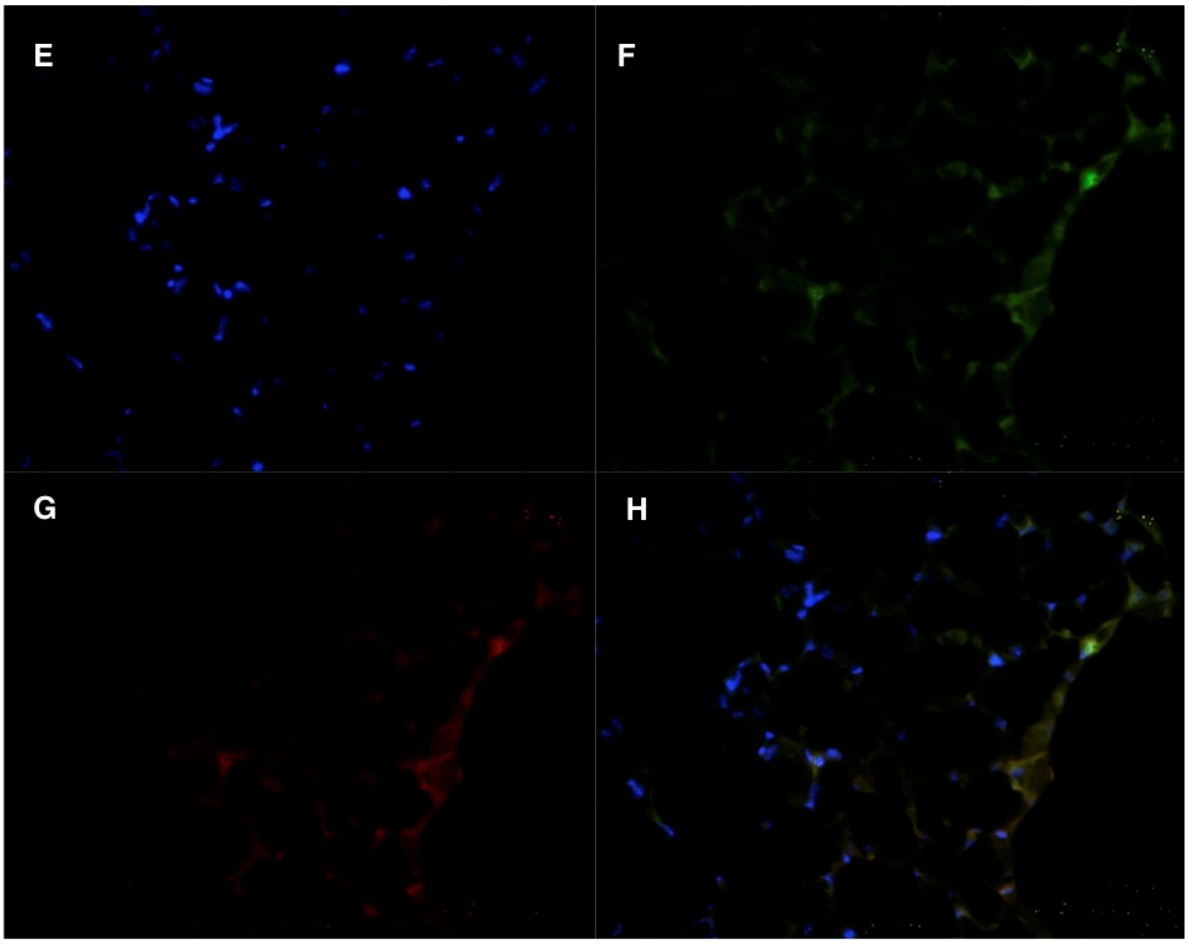
E
F
G
H